

Direct Urca process in a neutron star mantle

M. E. Gusakov¹, D. G. Yakovlev¹, P. Haensel², and O. Y. Gnedin³

¹ Ioffe Physical Technical Institute, Politekhnickeskaya 26, 194021 St. Petersburg, Russia
e-mail: yak@astro.ioffe.ru

² Copernicus Astronomical Center, Bartycka 18, 00-716 Warsaw, Poland
e-mail: haensel@camk.edu.pl

³ Space Telescope Science Institute, 3700 San Martin Drive, Baltimore, MD 21218, USA
e-mail: ognedin@stsci.edu

Received 17 February 2004 / Accepted 1 April 2004

Abstract. We show that the direct Urca process of neutrino emission is allowed in two possible phases of nonspherical nuclei (inverse cylinders and inverse spheres) in the mantle of a neutron star near the crust-core interface. The process is open because neutrons and protons move in a periodic potential created by inhomogeneous nuclear structures. In this way the nucleons acquire large quasimomenta needed to satisfy momentum-conservation in the neutrino reaction. The appropriate neutrino emissivity in a nonsuperfluid matter is about 2–3 orders of magnitude higher than the emissivity of the modified Urca process in the stellar core. The process may noticeably accelerate the cooling of low-mass neutron stars.

Key words. stars: neutron – dense matter

1. Introduction

It is well known (Lattimer et al. 1991) that direct Urca process produces the most powerful neutrino emission in the inner cores of neutron stars (NSs). The simplest direct Urca process in a dense degenerate matter, composed of neutrons (n) with an admixture of protons and electrons (p and e), consists of two successive reactions (direct and inverse ones):

$$n \rightarrow p + e + \bar{\nu}_e, \quad p + e \rightarrow n + \nu_e, \quad (1)$$

where ν_e and $\bar{\nu}_e$ are the electron neutrino and antineutrino, respectively. The process is allowed by momentum conservation if $p_{Fn} < p_{Fp} + p_{Fe}$, and forbidden otherwise. Here, p_{Fn} , p_{Fp} , and p_{Fe} are the Fermi-momenta of n, p, and e. The neutrino momentum $p_\nu \sim k_B T$ is much smaller than these Fermi momenta, and it can be neglected in momentum conservation (T is the internal NS temperature, and k_B is the Boltzmann constant). It turns out that the direct Urca process is allowed only at sufficiently high densities (typically, a few times of ρ_0 , where $\rho_0 = 2.8 \times 10^{14} \text{ g cm}^{-3}$ is the nuclear matter density at saturation) for those model equations of state of dense matter which have a large symmetry energy (rather high fractions of protons and electrons) to satisfy the inequality $p_{Fn} < p_{Fp} + p_{Fe}$.

Thus, the direct Urca process is forbidden in the cores of low-mass NSs. The main neutrino emission from these (nonsuperfluid) cores is produced by the modified Urca process

($nN \rightarrow pN\bar{\nu}_e$, $peN \rightarrow nN\nu_e$, where $N = n$ or p is a nucleon-spectator required for momentum conservation). The modified Urca process is 6–7 orders of magnitude weaker than the direct Urca process. This greatly reduces the neutrino emission of low-mass NSs in comparison with the emission of massive NSs, where the direct Urca is open.

In this paper we analyze the possibility to open the direct Urca process in the inner NS crust. The main idea is that a momentum excess may be absorbed by a lattice of nonuniform nuclear structures in the crust. Specifically, we consider a model of nonspherical nuclear structures which appear in the density range from $\rho \approx 10^{14} \text{ g cm}^{-3}$ to the crust-core interface ($\rho_{cc} \approx \rho_0/2$) if one employs some models of nucleon-nucleon interaction (Ravenhall et al. 1983; Pethick & Ravenhall 1995). The theory predicts a sequence of phase transitions with increasing ρ within this density range: from familiar spherical nuclei to cylindrical nuclear structures, from cylinders to slab-like structures, from slabs to inverted cylinders, then to inverted spheres and, finally (at $\rho = \rho_{cc}$), to a uniform nuclear matter in the core. The shell of nonspherical nuclei in the crust, sometimes called the *NS mantle*, is thin (not thicker than several hundred meters) but contains a noticeable fraction of the crust mass. We will consider two last phases – the inverted cylinders and the inverted spheres, where free protons appear (in addition to free neutrons in the inner crust), but periodic nuclear structures are still not dissolved into the uniform nuclear matter. The periodic structures modulate motion of neutrons and protons (inducing Bloch states) and open direct Urca process in a neutron-star mantle.

Send offprint requests to: M. E. Gusakov,
e-mail: gusakov@astro.ioffe.ru

2. Periodic potential and nucleon wave functions

In order to calculate the neutrino emissivity of direct Urca process in the NS mantle we need wave functions of neutrons and protons in a periodic nuclear potential. For understanding the main features of the problem, we adopt a simplified Thomas-Fermi approximation. The nuclear structures will be described using the results of Oyamatsu (1993). Specifically, we will employ his model I for the energy density functional. The potential energy of neutrons or protons ($j = n$ or p) can be calculated as

$$V_j(r) = \frac{\partial}{\partial n_j} \left\{ \epsilon_0(n_n, n_p) - \frac{3}{5} (3\pi^2)^{2/3} \left(\frac{\hbar^2}{2m_n} n_n^{5/3} + \frac{\hbar^2}{2m_p} n_p^{5/3} \right) \right\}, \quad (2)$$

where $\epsilon_0(n_n, n_p)$ is the energy density of the uniform nuclear matter, m_j is the nucleon mass, and $n_j(r)$ is a local number density of nucleon species j , which depends on distance r from the nucleus center inside a Wigner-Seitz cell (Eq. (4.8) of Oyamatsu 1993). Equation (2) neglects small gradient corrections. For simplicity, we restrict ourselves to scalar (spin-independent) nuclear potentials.

Using the Schrödinger perturbation theory we can express the Bloch wave function of a nucleon (n or p) in the periodical potential $V_j(r)$ as:

$$\Psi_p = \frac{\chi_s}{\sqrt{V}} \left(e^{i\mathbf{p}r} + \sum_{\mathbf{q} \neq 0} V_{j\mathbf{q}} \frac{e^{i\mathbf{p}'r}}{E_p - E_{p'}} \right) \equiv \frac{\chi_s}{\sqrt{V}} \sum_{\mathbf{q}} C_{\mathbf{q}} e^{i\mathbf{p}'r}, \quad (3)$$

where \mathbf{q} is an inverse lattice vector, $\mathbf{p}' = \mathbf{p} + \mathbf{q}$, V is the normalization volume, $C_0 = 1$, and $C_{\mathbf{q}} = V_{j\mathbf{q}}/(E_p - E_{p'})$ for $\mathbf{q} \neq 0$. Furthermore, χ_s is a unit spinor ($\chi_s \chi_{s'} = \delta_{ss'}$), $s = \pm 1$ is the sign of the nucleon spin projection onto the quantization axis, $E_p = \mathbf{p}^2/2m_j^*$ is the unperturbed energy, \mathbf{p}_j is the momentum, m_j^* is the effective mass at the Fermi surface, and $V_{j\mathbf{q}}$ is a Fourier-transform of the potential $V_j(r)$:

$$V_{j\mathbf{q}} = \frac{1}{V_{\text{cell}}} \int_{\text{cell}} V_j(r) e^{-i\mathbf{q}r} d\mathbf{r}, \quad (4)$$

V_{cell} being the elementary-cell volume. An exact calculation of $V_{j\mathbf{q}}$ is difficult because the configuration of the elementary cell is complicated. However, the calculation can be simplified due to the short-ranged character of nuclear forces. Consequently, the nucleon potential is almost constant near the cell boundaries, where it can be replaced by the boundary value V_∞ . Introducing a simplified Wigner-Seitz cell of equivalent volume as defined by Oyamatsu (1993), we find:

$$V_{j\mathbf{q}} = \frac{1}{V_{\text{WS}}} \int_{\text{cell}} (V_j(r) - V_\infty) e^{-i\mathbf{q}r} d\mathbf{r} \approx \frac{1}{V_{\text{WS}}} \int_{\text{WS}} (V_j(r) - V_\infty) e^{-i\mathbf{q}r} d\mathbf{r}, \quad (5)$$

where we have used the identity

$$\int_{\text{cell}} e^{-i\mathbf{q}r} d\mathbf{r} = 0. \quad (6)$$

Now in Eq. (5) we can integrate over the simplified Wigner-Seitz cell (a cylinder or a sphere for the phases of inverted cylinders and inverted spheres, respectively).

Unless the contrary is indicated, we will use the units, where $\hbar = c = k_B = V = 1$. Notice, that the perturbation expansion (3) fails (becomes singular) at Bragg's diffraction points (at $|\mathbf{p}| = |\mathbf{p} + \mathbf{q}|$) which signals the special importance of the band structure near these points. However, we will see that nucleons with such "resonant" wave functions do not contribute to the neutrino process of study.

3. General formalism

The emissivity Q of the direct Urca process in a NS mantle is calculated in the same way as in a NS core (Lattimer et al. 1991). Using the notations from the review article by Yakovlev et al. (2001), we obtain:

$$Q = 2 \int \frac{d\mathbf{p}_n}{(2\pi)^3} dW_{i \rightarrow f} \epsilon_\nu f_n (1 - f_p) (1 - f_e), \quad (7)$$

where f_j is the Fermi-Dirac distribution of particle species j ($j = n, p, e$), ϵ_ν is the neutrino energy, $dW_{i \rightarrow f}$ is the differential probability of neutron decay (calculated with the wave functions (3)). The overall factor 2 doubles the emissivity of the neutron decay to account for the contribution of the inverse reaction (assuming β -equilibrium). After standard simplifications (e.g., Yakovlev et al. 2001) and integration over orientations of the neutrino momentum, we get:

$$dW_{i \rightarrow f} \frac{d\mathbf{p}_n}{(2\pi)^3} = \frac{(2\pi)^4}{(2\pi)^{12}} \sum_{\mathbf{q}_n, \mathbf{q}_p} \delta(\epsilon_n - \epsilon_p - \epsilon_e - \epsilon_\nu) \times \delta(\mathbf{p}'_n - \mathbf{p}'_p - \mathbf{p}_e) \times |M_{fi}|^2 4\pi \epsilon_\nu^2 d\epsilon_\nu \prod_{j=1}^3 p_{F_j} m_j^* d\epsilon_j d\Omega_j, \quad (8)$$

where ϵ_j is the energy of particle species j , $d\Omega_j$ is the solid angle element in the direction of \mathbf{p}_j , $|\mathbf{p}_j| = p_{F_j}$ (i.e., nonperturbed particle momenta \mathbf{p}_j in the momentum-conserving delta function are placed at Fermi surfaces), and $m_e^* = \mu_e$ (μ_e being the electron chemical potential). Finally,

$$|M_{fi}|^2 = 2 G_F^2 \cos^2 \theta_C |C_{q_n}|^2 |C_{q_p}|^2 (f_V^2 + 3g_A^2) \quad (9)$$

is the squared matrix element, summed over particle spins and averaged over directions of neutrino momentum. Here, $G_F = 1.436 \times 10^{-49}$ erg cm³ is the Fermi weak interaction constant, θ_C is the Cabibbo angle, $\sin \theta_C = 0.231$, $f_V = 1$ is the vector interaction constant, and $g_A = 1.26$ is the Gamow-Teller axial-vector interaction constant.

The leading term in the sum (8) over inverse lattice vectors corresponds to $\mathbf{q}_n = \mathbf{q}_p = 0$. However, in this term $\mathbf{p}'_n = \mathbf{p}_n$, $\mathbf{p}'_p = \mathbf{p}_p$ (see Eq. (3) and the discussion afterwards), and the neutrino emission is forbidden ($p_{Fn} \geq p_{Fp} + p_{Fe}$) by momentum conservation. Thus, the main contribution into the emissivity Q comes from smaller terms with either $\mathbf{q}_n = 0$ or $\mathbf{q}_p = 0$. The terms with $\mathbf{q}_n \neq 0$ and $\mathbf{q}_p \neq 0$ are even smaller and can be neglected. The retained terms are constructed in such a way that the momentum-conserving delta function excludes the "dangerous" Bragg diffraction points. For instance, one can easily show that for $\mathbf{q}_n = 0$ the Bragg diffraction condition $|\mathbf{p}_p| = |\mathbf{p}_p + \mathbf{q}_p|$ is incompatible with momentum conservation in Eq. (8).

Inserting Eq. (8) into Eq. (7) and integrating over particle energies and propagation directions, we get:

$$Q(T, \rho) = Q_0(T, \rho) R(\rho), \quad (10)$$

$$Q_0(T, \rho) = \frac{457\pi}{10080} G_F^2 \cos^2 \theta_C \left(f_V^2 + 3g_A^2 \right) m_n^* m_p^* m_e^* T^6 \\ \approx 4.0 \times 10^{27} \left(\frac{n_e}{n_0} \right)^{1/3} \frac{m_n^* m_p^*}{m_n m_p} T_9^6 \frac{\text{erg}}{\text{cm}^3 \text{ s}}, \quad (11)$$

$$R(\rho) = \sum_{j=n,p} \sum_q \frac{(m_j^* V_{jq})^2}{\alpha_j p_{Fj}^4} \\ \times \left[F(2\alpha_j D_j^{\max} + \alpha_j^2) - F(2\alpha_j D_j^{\min} + \alpha_j^2) \right], \quad (12)$$

where n_e is the electron number density, $n_0 = 0.16 \text{ fm}^{-3}$ is the nucleon number density in saturated nuclear matter, $T_9 = T/10^9 \text{ K}$, $\alpha_j = q/p_{Fj}$, $D_j^{\min} = \max(-1, D_{j-})$, $D_j^{\max} = \min(1, D_{j+})$. Furthermore,

$$F(x) = \frac{1}{2} \ln \left| \frac{\sqrt{1+x+1}}{\sqrt{1+x-1}} \right| - \frac{\sqrt{1+x}}{x},$$

$$D_{n\pm} = \frac{(p_{Fp} \pm p_{Fe})^2 - p_{Fn}^2 - q^2}{2p_{Fn}q},$$

$$D_{p\pm} = \frac{(p_{Fn} \pm p_{Fe})^2 - p_{Fp}^2 - q^2}{2p_{Fp}q},$$

for $p_{Fn} - p_{Fp} - p_{Fe} \leq q \leq p_{Fn} + p_{Fp} + p_{Fe}$ (and $F(x) = 0$ otherwise). In Eq. (10) Q_0 is the direct Urca emissivity in the uniform nuclear matter (disregarding the momentum-conservation constraint) and R can be called its *reduction factor* which describes the weakening of the process in the NS mantle. This factor depends on ρ , but not on T . The emissivity Q is $\propto T^6$, just as for the well-known direct Urca process in the NS core.

For calculating R from Eq. (12) we need the particle Fermi-momenta. Because our analysis is simplified, we have used two models. *First*, we have defined the Fermi-momenta by:

$$p_{Fn} = (3\pi^2 n_n)^{1/3}, \quad p_{Fp} = p_{Fe} = (3\pi^2 n_p)^{1/3}, \quad (13)$$

where n_n and n_p are the nucleon number densities averaged over the Wigner-Seitz cell (see Eq. (4.8) and Table 6 of Oyamatsu 1993), and $p_{Fp} = p_{Fe}$ due to electric neutrality. *Second*, we have adopted electric neutrality and β -equilibrium, and determined the Fermi-momenta from the equations:

$$p_{Fe} = p_{Fp}, \quad \frac{p_{Fn}^2}{2m_n} + V_{n0} = \frac{p_{Fp}^2}{2m_p} + V_{p0} + p_{Fe}, \quad (14)$$

where V_{j0} is the central ($\mathbf{q} = \mathbf{0}$) Fourier harmonics of the nucleon potential $V_j(r)$.

The values of $R(\rho)$ calculated from Eq. (12) appear to be qualitatively the same for both models. In our calculations we have set $m_j^* = m_j$, but variations of m_j^* within reasonable limits do not qualitatively change $R(\rho)$. The results based on the model (14) can be fitted by

$$R(\rho) \approx R_2 + (R_1 - R_2)(1 - x)^2 \quad x < 1, \\ R(\rho) \approx R_2/x^7 \quad x \geq 1, \quad (15)$$

where $R_1 = 6 \times 10^{-5}$, $R_2 = 10^{-5}$, $x = (n_b - n_1)/(n_2 - n_1)$, $n_b = \rho/m_n$ is the baryon number density, while n_1 and n_2 are the baryon number densities at the outer and inner boundaries of the inverted-cylinder phase. Thus, the density parameter x varies from 0 to 1 in the layer of inverted cylinders, and we have $x > 1$ in the layer of inverted spheres. In the Oyamatsu model, which we employ, $n_1 = 0.08274 \text{ fm}^{-3}$, $n_2 = 0.08537 \text{ fm}^{-3}$, and the layer of inverted spheres extends to $n_3 = 0.08605 \text{ fm}^{-3}$ (to $x = 4.868$).

The number N of inverted lattice vectors, which contribute into R , is large: $N \sim 200$ for the phase of inverted cylinders, and N is up to ~ 2800 for the phase of inverted spheres. The proton contribution ($\mathbf{q}_p \neq \mathbf{0}$) into R is approximately three times larger than the neutron one ($\mathbf{q}_n \neq \mathbf{0}$).

As seen from Eq. (15), $R \sim 10^{-5}$. Thus, the emissivity of the direct Urca process in the mantle is about 5 orders of magnitude weaker than in the inner NS core. Nevertheless, as will be shown in the next section, the direct Urca in the mantle can affect the cooling of NSs.

4. The effect on the cooling of low-mass NSs

We will focus on sufficiently low-mass NSs, with the forbidden direct Urca process in the inner cores (Sect. 1). The cooling behaviour of these stars is described, for instance, by Potekhin et al. (2003). The neutrino luminosity L_ν of low-mass stars is not too high. Thus, the additional neutrino emission from the mantle may be pronounced at the neutrino cooling stage (when the stellar age $t \lesssim 10^5 \text{ yr}$).

An order-of-magnitude estimate gives

$$L_\nu \sim 4\pi R_{cc}^2 h Q + (4\pi/3) R_{cc}^3 Q_{\text{core}}, \quad (16)$$

where R_{cc} is the core radius, h is the mantle width, and Q_{core} is the mean neutrino emissivity from the NS core. Adopting $R_{cc} = 10 \text{ km}$ and $h = 100 \text{ m}$, we obtain that the direct Urca in the mantle may affect the cooling if $Q \gtrsim 30 Q_{\text{core}}$, which is quite possible. For instance, this inequality may hold for non-superfluid low-mass NSs. The main neutrino emission in the cores of these NSs is produced by the modified Urca process, which is 6–7 orders of magnitude weaker than the direct Urca process in the cores of massive NSs, while the direct Urca process in the mantle is five orders of magnitude weaker than in the cores of massive NSs.

Let us illustrate these statements by more elaborated calculations. For this purpose we employ the equation of state of Prakash et al. (1988) in the stellar cores (the version with the compression modulus of the saturated symmetric nuclear matter $K = 240 \text{ MeV}$ and with model I for the symmetry energy). The NS models based on this equation of state are described, e.g., by Yakovlev et al. (2001). The equation of state opens direct Urca process in the NS core at $\rho \geq 7.85 \times 10^{14} \text{ g cm}^{-3}$ (which is possible in NSs with $M > 1.358 M_\odot$). The most massive stable NS has the central density $\rho_c = 2.578 \times 10^{15} \text{ g cm}^{-3}$ and the mass $M = 1.977 M_\odot$. A typical low-mass NS with $M = 1.35 M_\odot$ has $\rho_c = 7.79 \times 10^{14} \text{ g cm}^{-3}$ and $R = 13.0 \text{ km}$.

We have simulated NS cooling with our fully relativistic cooling code (Gnedin et al. 2001). It calculates the cooling

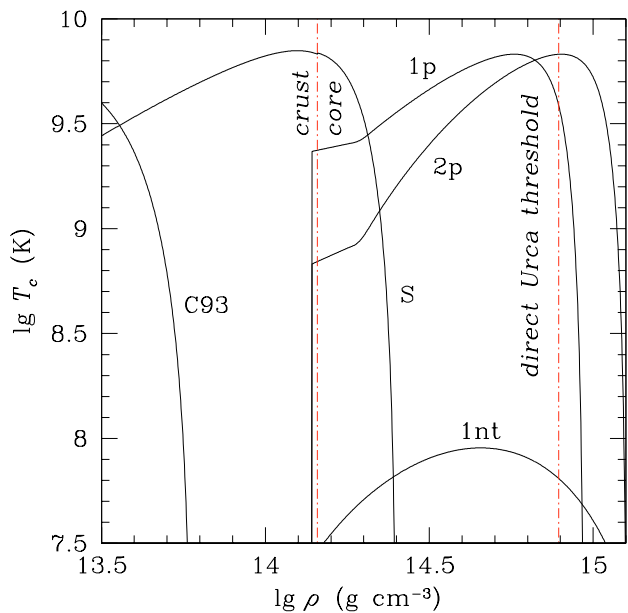


Fig. 1. Critical temperature T_c versus ρ for various models of neutron and proton pairing in the NS core and crust. Models C93 and S: singlet-state neutron pairing in the crust; models 1p and 2p: singlet-state proton pairing in the core; model 1nt: weak triplet-state neutron pairing in the core. The crust-core interface and the threshold density of the direct Urca process in the core are shown by vertical dot-and-dashed lines.

curves: the NS surface temperature T_s^∞ , as detected by a distant observer, versus the NS age t . We have updated the code by incorporating the neutrino emission from the direct Urca process in the NS mantle. We have considered nonsuperfluid NSs and NSs with neutron and proton superfluidity of the internal layers. We have taken into account (i) a possible singlet-state pairing of free neutrons in the crust and the outermost part of the core; (ii) a triplet-state pairing of neutrons in the core; and (iii) a singlet-state pairing of protons in the crust.

Microscopic theories of nucleon superfluidity of dense matter give very model dependent density profiles of superfluid critical temperatures of nucleons, $T_c(\rho)$ (e.g., Lombardo & Schulze 2001). Thus, we have considered several superfluid models (Fig. 1) available in the literature: one phenomenological model 1p of strong singlet-state proton pairing, and one phenomenological model 1nt of weak triplet-state neutron pairing in the NS core (Kaminker et al. 2002); models S (Schulze et al. 1996) and C93 (Chen et al. 1993) of singlet-state neutron pairing in the crust. We have also proposed the additional phenomenological model 2p of proton pairing in the core (not to be confused with model 2p in Kaminker et al. 2002!). This pairing is rather weak at the core-crust interface but becomes much stronger at higher ρ .

The effects of superfluidity on the neutrino emission and heat capacity of the matter have been included in the standard way (Yakovlev et al. 1999). It is well known that the nucleon superfluidity reduces the traditional neutrino mechanisms but opens the neutrino emission due to Cooper pairing of nucleons. We assume that free protons and free neutrons in the mantle have the same $T_c(\rho)$ as protons in the core and free

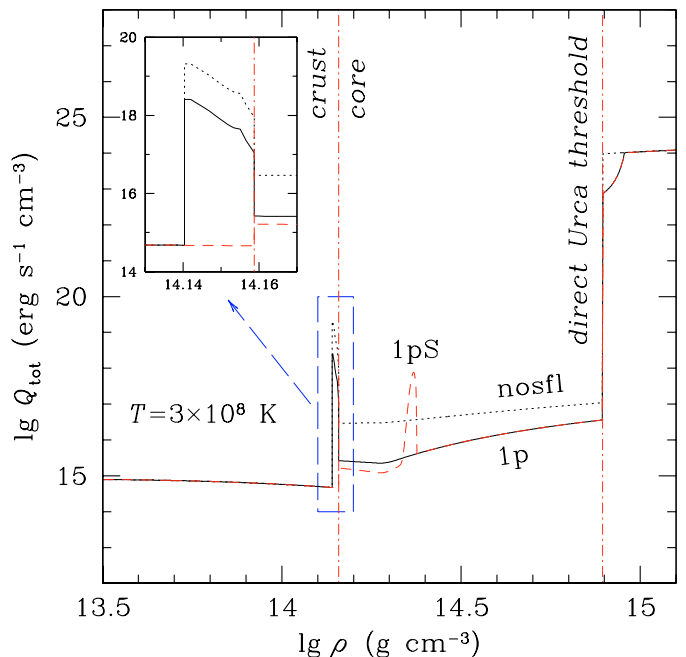


Fig. 2. Total neutrino emissivity versus density at $T = 3 \times 10^8$ K. The crust-core interface and the direct Urca threshold in the core are marked by dot-and-dashed lines. The peak near the core-crust interface shows the direct Urca process in the mantle (also presented in the insert). Dotted line: no nucleon superfluidity (nosfl); solid line: model 1p of proton superfluidity; dashed line: model 1p of proton superfluidity in the core and model S of neutron superfluidity in the crust (see the text). The neutron pairing 1nt is too weak to appear and affect the neutrino emission at the given T .

neutrons in the ordinary crust of spherical nuclei. We have adopted the same form of the superfluid reduction factor of the direct Urca process in the mantle as in the inner core.

Figure 2 shows the density profile of the total neutrino emissivity at $T = 3 \times 10^8$ K for nonsuperfluid and superfluid NSs, while Fig. 3 presents some cooling curves. All the curves, but one short-dashed curve, are calculated for a $1.35 M_\odot$ NS with the forbidden direct Urca process in the core. This is a typical example of a low-mass NS. Any pair of lines of the same type corresponds to the same superfluidity model. Every upper line of the pair is calculated neglecting the direct Urca process in the mantle while its lower counterpart is calculated including this process. The short dashed curve is an example of the cooling of a more massive, $1.5 M_\odot$, nonsuperfluid NS. Its central density is $\rho_c = 9.0 \times 10^{14} \text{ g cm}^{-3}$; the direct Urca process is open in the inner stellar core, producing a strong neutrino emission and a rapid cooling of the star. In this case the direct Urca process in the mantle is entirely negligible: it cannot compete with its senior partner in the core.

Along with the theoretical curves, in Fig. 3 we present the observational limits on the effective surface temperatures and ages of two NSs, RX J0822–4300 and PSR B1055–52. Among all middle-aged isolated NSs, whose thermal emission has been observed and the effective surface temperature measured (the data are given, e.g., in Yakovlev et al. 2004), these are the NSs hottest for their ages. They can be interpreted as

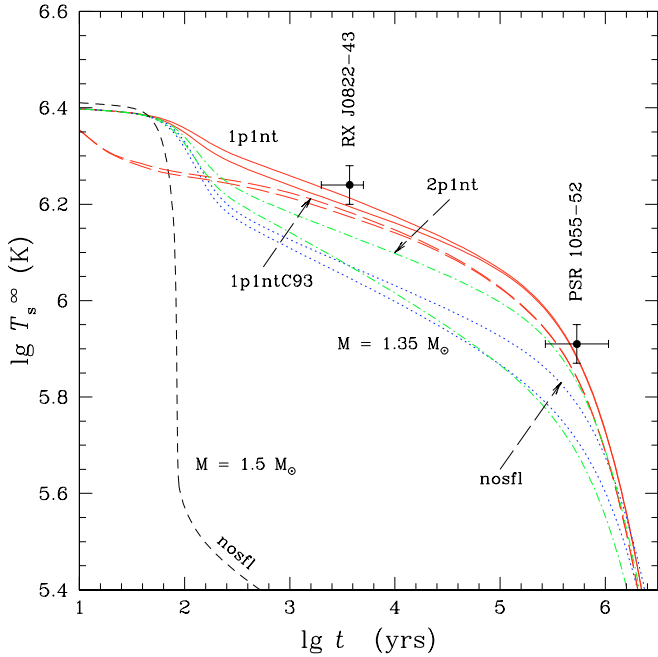


Fig. 3. Theoretical cooling curves compared with observations of two NSs. All the lines but the short-dashed one are for $1.35 M_{\odot}$ NS (direct Urca in the core forbidden). Any pair of lines of the same type refers to one superfluidity model with the direct Urca process in the mantle on (lower curve) or off (upper curve). Dotted curves: nonsuperfluid NSs (nosfl); solid curves: 1p and 1nt superfluidities in the core; long dashes: 1p and 1nt superfluidity in the core and C93 superfluidity of neutrons in the crust; dot-and-dash lines: 2p and 1nt superfluidities in the core. The short dashed line is for a nonsuperfluid $1.5 M_{\odot}$ NS with the open direct Urca process in the core.

low-mass NSs (see, e.g., Yakovlev et al. 2004 and references therein).

RX J0822–4300 is a radio silent NS, a compact central object in Puppis A. Its effective temperature is taken from Zavlin et al. (1999). Recently Pavlov (2003) has kindly provided us with the updated value of the effective temperature of PSR B1055–52, $T_s^{\infty} \approx 7 \times 10^5$ K. However, he has not indicated errorbars. We introduce (Fig. 3), somewhat arbitrarily, 10% uncertainties of T_s^{∞} . The ages of RX J0822–4300 and PSR B1055–52 are taken as described by Yakovlev et al. (2004).

The dotted line in Fig. 2 shows the neutrino emissivity in a nonsuperfluid NS. The peak before the crust-core interface is produced by the direct Urca process in the mantle (additionally presented in the insert). The emissivity at the peak maximum is about three orders of magnitude larger than in the NS core. The appropriate cooling curves are shown by the dotted lines in Fig. 3. The direct Urca process in the mantle noticeably accelerates the cooling at $t \sim 10^5$ yr.

Assuming the strong 1p proton pairing and the weak 1nt triplet-state neutron pairing in the core (and the mantle) but no singlet-state neutron pairing in the crust, we obtain the emissivity profile plotted by the solid line in Fig. 2. The proton superfluidity fully suppresses the modified Urca process in the outer core, before the direct Urca threshold, and partly suppresses the direct Urca process in the inner core (of massive NSs) beyond

the threshold. The neutron pairing in the core is so weak that it does not appear at $T = 3 \times 10^8$ K in Fig. 2. The neutrino emission from the core of a low-mass NS becomes very slow, being mainly determined by the neutron-neutron bremsstrahlung process. This increases the surface temperatures of middle-aged NSs (the solid curves in Fig. 3), and enables one to interpret the observations of RX J0822–4300 and PSR B1055–52 (e.g., Kaminker et al. 2002; Yakovlev et al. 2004). In this case the proton superfluidity partly suppresses the direct Urca process in the mantle and reduces the difference of the cooling curves calculated with and without this process. Notice that the combination of the superfluidities 1p and 1nt is sufficient to explain the data on all isolated middle-aged NSs (whose surface temperatures have been measured (estimated) from the observations of their thermal radiation) by theoretical cooling curves of NSs with different masses (e.g., Kaminker et al. 2002). We see that the inclusion of the direct Urca process in the mantle does not violate this interpretation.

If we additionally switch on the singlet-state superfluidity C93 in the crust, we will obtain the long-dashed cooling curves in Fig. 3, which go slightly lower than the solid curves. This additional acceleration of the cooling is produced by the neutrino emission due to Cooper-pairing of neutrons in the crust. The effect is weak because the superfluidity C93 dies out long before the crust-core interface and produces the weak Cooper-pairing emission (Potekhin et al. 2003). The relative importance of the direct Urca process in the mantle is even lower than in the absence of the superfluidity C93.

If we add the singlet-state neutron superfluidity S instead of C93, the situation would be different in two respects. First, the superfluidity S completely switches off the direct Urca process in the mantle (see the dashed curve in Fig. 2; its peak in the core is produced by the neutrino emission due to the pairing S). Second, the superfluidity S occupies much larger fraction of the NS volume than the superfluidity C93, intensifying the neutrino emission due to the singlet-state pairing of neutrons. Now this emission noticeably lowers the cooling curve, complicating the interpretation of RX J0822–4300 and PSR B1055–52. We do not present the cooling curve for that unlikely case in Fig. 3; it is the same as given by Potekhin et al. (2003).

Finally, let us employ the proton pairing 2p and the neutron pairing 1nt in the core (and neglect the singlet-state neutron pairing in the crust). The proton superfluidity 2p suppresses the neutrino emission in the main fraction of the core but not in the mantle. The effect of the direct Urca process in the mantle on the cooling of NSs of the age $t \sim (10^4-10^5)$ yr becomes most pronounced (the dot-and-dash curves in Fig. 3). With this process on (the lower dot-and-dash curve) the low-mass star will cool too fast, strongly complicating the interpretation of the observations of RX J0822–4300 and PSR B1055–52.

Let us emphasize that the existence of the NS mantle (the layer of nonspherical atomic nuclei) is still a hypothesis. The theory predicts this layer only within some models of nucleon-nucleon interaction. Since the lower dot-and-dash curve in Fig. 3 strongly contradicts the observations, the underlying physical scenario becomes doubtful. This would imply, for instance, that the 2p proton superfluidity model is inadequate, or

the neutrons in the mantle are strongly superfluid (switching off the direct Urca process), or the mantle does not exist at all.

Our analysis of cooling low-mass NSs is illustrative and incomplete. The cooling of these NSs is actually affected by (i) NS superfluidity; (ii) NS surface magnetic fields; and (iii) possible surface layer of light (accreted) elements (as discussed in detail by Potekhin et al. 2003). Our calculations indicate the existence of the fourth regulator; (iv) the presence of the NS mantle and the associated direct Urca process. As clear from the results of Potekhin et al. (2003) and our present results, *all four regulators are of comparable strength* and should be analyzed together. This many-parametric analysis is beyond the scope of the present article.

5. Conclusions

We have calculated the neutrino emissivity of the new neutrino mechanism – the direct Urca process in a neutron-star mantle, a thin layer of nonspherical nuclei (Ravenhall et al. 1983; Pethick & Ravenhall 1995) adjacent to the stellar core. The mantle is predicted only by some models of nucleon-nucleon interaction (and is not predicted by other models). Thus, the existence of the mantle is hypothetical. If exists, it cannot noticeably affect the equation of state, and the hydrostatic NS structure (particularly, NS masses and radii). We expect that the strongest manifestation of the mantle consists in opening direct Urca process. It can operate in the two last phases of nonspherical nuclei (inverted cylinders and inverted spheres), where the continuum proton spectrum is formed (e.g., Oyamatsu 1993). The emissivity of the new process in a nonsuperfluid mantle appears to be 2–3 orders of magnitude higher than the neutrino emissivity in the nonsuperfluid outer NS core.

We have performed illustrative calculations of NS cooling which show that the new process can noticeably affect the cooling of low-mass NSs. Its effect is most pronounced in NSs with strongly superfluid cores (to reduce the neutrino emission from the cores) and nonsuperfluid mantles (to fully open direct Urca process there). Thus, direct Urca process in the mantle represents a new regulator of the cooling of low-mass NSs.

Our calculation of the emissivity of the new process is simplified (based on the Thomas-Fermi model with a simplified form of scalar nucleon interaction, and an approximate choice of nucleon Fermi momenta). The calculation can be improved but we expect that the main results will be qualitatively the same. One cannot exclude (Jones 2001) that direct Urca process operates also in the crust of spherical atomic

nuclei, or in some selected layers of the crust, but its calculation is difficult (requires exact wave functions of nucleons). If operates, it could be a stronger regulator of NS cooling than direct Urca process in the mantle.

It is important that delicate properties of subnuclear matter can potentially be tested by observations of cooling NSs. As clear from our discussion, NSs hottest for their ages are the most suitable targets of such tests.

Acknowledgements. This work was supported in part by the RFBR (grants 02-02-17668 and 03-07-90200), the RLSS (grant 1115.2003.2), KBN (grant 5 P03D 020 20), and by the INTAS (grant YSF 03-55-2397).

References

- Chen, J. M. C., Clark, J. W., Davé, R. D., & Khodel, V. V. 1993, *Nucl. Phys. A*, 555, 59
- Gnedin, O. Y., Yakovlev, D. G., & Potekhin, A. Y. 2001, *MNRAS*, 324, 725
- Jones, P. B. 2001, *MNRAS*, 321, 167
- Kaminker, A. D., Yakovlev, D. G., & Gnedin, O. Y. 2002, *A&A*, 383, 1076
- Lattimer, J. M., Pethick, C. J., Prakash, M., & Haensel, P. 1991, *Phys. Rev. Lett.*, 66, 2701
- Lombardo, U., & Schulze, H.-J. 2001, in *Physics of Neutron Star Interiors*, ed. D. Blaschke, N. K. Glendenning, & A. Sedrakian (Berlin: Springer), 30
- Oyamatsu, K. 1993, *Nucl. Phys. A*, 561, 431
- Pavlov, G. G. 2003, private communication
- Pethick, C. J., & Ravenhall, D. G. 1995, *Ann. Rev. Nucl. Part. Sci.*, 45, 429
- Potekhin, A. Y., Yakovlev, D. G., Chabrier, G., & Gnedin, O. Y. 2003, *ApJ*, 594, 404
- Prakash, M., Ainsworth, T. L., & Lattimer, J. M. 1988, *Phys. Rev. Lett.*, 61, 2518
- Ravenhall, D. G., Pethick, C. J., & Wilson, J. R. 1983, *Phys. Rev. Lett.*, 50, 2066
- Schulze, H.-J., Cugnon, J., Lejeune, A., Baldo, M., & Lombardo, U. 1996, *Phys. Lett. B*, 375, 1
- Yakovlev, D. G., Levenfish, K. P., & Shibunov, Yu. A. 1999, *Physics – Uspekhi*, 42, 737
- Yakovlev, D. G., Kaminker, A. D., Gnedin, O. Y., & Haensel, P. 2001, *Phys. Rept.* 354, 1
- Yakovlev, D. G., Gnedin, O. Y., Kaminker, A. D., Levenfish, K. P., & Potekhin, A. Y. 2004, *Adv. Space Res.*, 33, 523
- Zavlin, V. E., Trümper, J., & Pavlov, G. G. 1999, *ApJ*, 525, 959